Sultan Qaboos University
Deanship of Research
Research Department

(A) Project Details

Project Code:	IG/ENG/MIED/18/02		
Project Title:	Development of Precise Sensorless Piezo-actuated Nanopositioning Systems		
College/Center:	Engineering	Department:	Mechanical and Industrial
Project Start Date:	01/01/2018	Project End Date:	30/12/2019
Date of Submission:	16/01/2020		
Research Team			
Principal Investigator:	Morteza Mohammadzaheri	SQU ID No.: 12252	
	Academic Ranking: Assistant Prof	Email: morteza@squ.edu.om	
Co-Principal Investigator:	Mojtaba Ghodsi	SQU ID No.: 10918	
	Academic Ranking: Assistant Prof	Email: ghodsi@squ.edu.om	
Co-Investigators (list all co-investigators):	Issam Bahadur, Assistant Prof, Mechanical and Industrial Engineering Musaab Zarog, Assistant Prof, Mechanical and Industrial Engineering		

(B) Budget (OMR)

Total Amount Allocated for the Project	Actual Expenditure	Balance
5000		

(C) External Fund/Support

Please list all funds/support the project received from sponsors over the past year (*if applicable*).

Sponsor	Funds/Support Amount

(D) Technical Report

Executive summary: Please detail the progress that has been made on the project (*min 500 words*)

The project aimed at design of a precise sensorless nanopositioning systems with use of piezoelectric actuators. Nanopositioning has a wide variety of high tech applications. The major task in nanopositioning is to control displacement/position of the actuator. Piezoelectric actuators are the most precise actuators for nanopositioning. Feedback position control systems need displacement/position sensors, and these sensors are the major source of cost and operation limit in nanopositioning systems. For example, a capacitive displacement sensor (to be used for nanopositioning) is almost 20 times more expensive than a regular piezoelectric actuator. In addition, a lot of space, time and effort is needed to use these sensors.

It is known, since 1982, that for a wide operating area, charge of a piezoelectric actuator is proportional to its position. That is, a precise charge estimator can play the role of a displacement/position sensor. This research made a major progress in this area. The first practical charge estimator of piezoelectric actuators, for nanopositioning purposes, was introduced in 2006, with a capacitor in series with the actuator. However, in such a systems, a large portion of the applied voltage is taken by the aforementioned capacitor, namely voltage drop. Voltage drop is not used in excitation of the actuator. In 2010, a resistor (known as the sensing resistor) was suggested to replace the capacitor. This new method needed a digital processor for calculations (along with other components listed in Methodology). These charge estimators of piezoelectric actuators with sensing resistor (CEPASRs) showed smaller voltage drops and are being further developed. However, all reported CEPASR, before this project, used a fixed resistor for the entire operating area.

During research sponsored by this internal grant, the investigators first identified a rigorous design guideline/criterion for CEPASRs: the range of V_S should be equal to the smallest input range of the analogue to the employed digital (A/D) converter. This guideline guarantees the maximum precision at the smallest possible voltage drop, as discussed in detail in Methodology section. Then, the investigators found that with a fixed resistor this guideline cannot be met for a wide operating area, as clearly shown in Figs. 2 and 3 in Methodology section. Thus, the idea of adaptive CEPASR was proposed: change of the sensing resistor with change of operating conditions.

Design of an adaptive CEPASR requires an algorithm to approximate the sensing resistor so that the aforementioned design guideline is met. This approximation problem was tackled with two approaches: analytical modelling and data driven modelling. Analytical modelling is based on the assumption that the piezoelectric can be approximated as a capacitor. The developed analytical model overestimates the sensing resistor in all operating area. As detailed in Methodology section, overestimation leads to loss of access to charge data for period of time, due to saturation of A/D converter, a serious consequence. Eight different data-driven methods were tried in this research including five Artificial Intelligence (AI) methods and three statistical methods. AI methods include Mutli Layer Perceptrion (MLP), Neurofuzzy network, Fully Connected Cascade (FCC) network and exact and efficient Radial Basis Function Network (RBFN). Statistical methods include linear modelling, cubic interpolation and averaging. MLP presented the best

approximation of the sensing resistance. However, in order to reduce the chance of overestimation to 1%, it is suggested to deduct MLP output from (3 ×estimation standard deviation+ estimation bias). With use of accurately approximated sensing resistors, a sensorless control systems was designed and implemented.

Introduction & Literature Review

Nanopositioning is a core aspect of nanotechnology, aiming at control of motion at nanometre scale. This area of technology has various applications such as scanning probe microscopy [1] (e.g. atomic force microscopy [2]), cell manipulation [3], robotic surgery [4] and ultra-fine machining [5]. Different actuators have been used for nano/micropositioning e.g. worm gears [6], magnetostrictive actuators [7] and linear motors [8]. Amongst all, piezoelectric actuators are the least bulky and the most precise ones [9]. They are currently the most common actuators for nanopositioning and are likely to maintain this status for years [10].

The major task in piezo-actuated nanopositioning is accurate position control of (an unfixed point/surface of) the actuator [11]. The origin of (a point/surface) position is the location (of the same point/surface) when the actuator has not been subject to any excitation for a reasonably long period of time (e.g. some minutes), i.e. a piezoelectric actuator's position is its displacement from relaxing state. However, measurement of position needs costly and difficult to operate sensors [12]. An alternative is to estimate position based on easy to measure signals. There are three signals which may be of use for this purpose: 'charge' of the actuator, the voltage across the actuator or 'piezoelectric voltage', and the voltage induced in actuator electrodes, or 'induced voltage'. The latter is only applicable for piezoelectric tubes and has been shown that its use is not beneficial when piezoelectric voltage is available [13]. Piezoelectric voltage has major drawback: the relationship between an actuator's position and its piezoelectric voltage is nonlinear, complex and still under investigation [14-16]. A pioneer work reported that such nonlinearities can cause up to 40% error in position control of piezoelectric actuators [17]. On the other hand, experiments have indicated that charge of a piezoelectric actuator is proportional to its position for a wide area of operating [18-21]. That is, a charge estimator can replace a relatively expensive and troublesome position/displacement sensor. This possibility has motivated design of charge estimators for piezoelectric actuators [9, 22, 23].

All existing charge estimators need electrical element(s) (e.g. resistor(s) or capacitor(s)) in series with the piezoelectric actuator [14]. These elements take a portion of the excitation voltage. This portion, the voltage across the aforesaid elements, is not used to expand/contract the actuator. Such squandered voltage is called 'voltage drop'[20]. Bazghaleh et al, showed that charge estimators with sensing resistor have the least voltage drop among existing charge estimators of piezoelectric actuators [21]. Thus, these estimators are investigated and further developed in this research. Charge estimators of piezoelectric actuators with sensing resistor (CEPASRs) are widely called "digital charge estimators" [24], because , unlike other estimators, they cannot be implemented without digital processors.

CEPASRs often use a fixed sensing resistor, e.g. [12, 21, 25]. In Methodology section of this report, it is manifestly shown that such estimators encounter either a significant voltage drop or impreciseness dealing with extensive operating areas. Then, the observed dilemma is investigated, formulated and tackled.

Methodology

1- Piezo-actuated Nanopositioning Systems with CEPASR

A number of piezo-actuated nanopositioning systems with CEPASR have been developed since 2010, e.g. the ones reported in [19, 21, 26]. Figure 1 is a schematic of a nanopositioning system with CEPASR, which works in operating areas where charge is proportional to position, or $q_P = K_{dc}\, d$ (1)
where q_P and d stand for piezoelectric actuator charge and position.

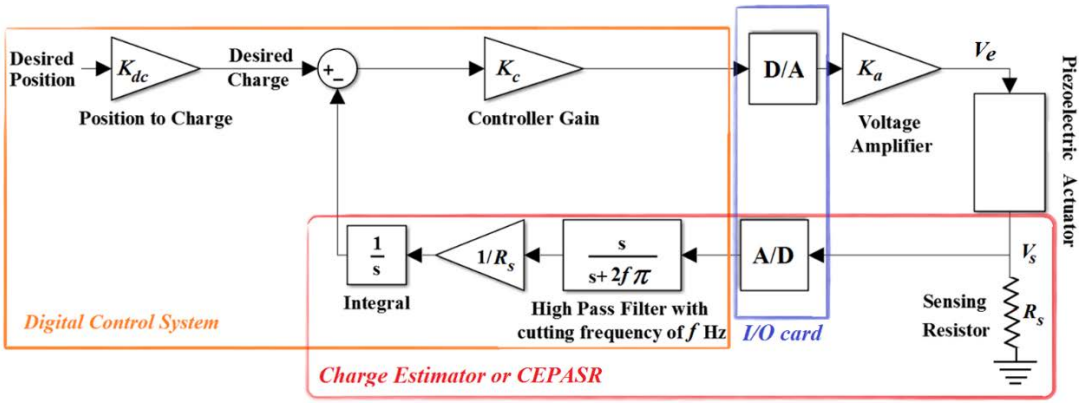

Figure 1. A schematic of a piezo-actuated nanopositioning system with CEPASR. A/D (D/A) refer to analogue (digital) to digital (analogue) converter.

In analogue part (outside the digital control system), almost entire current passing the actuator, i_P, passes through the grounded sensing resistor, R_S, and only a very minute current enters the digital controller:

$$i_P \simeq \frac{V_S}{R_S}, \tag{2}$$

where V_S is the voltage across the sensing resistor: the sensing voltage. As a result, in Fig.1, if high pass filter is neglected, the voltage after block $1/R_S$ equals i_P, and its integral equals charge of the actuator. This charge is compared to the desired charge, and the error is fed to a voltage amplifier which plays the role of a P-action controller.

However, charge estimation faces an issue in practice: a nearly constant (low frequency) small bias voltage, V_b , happens to be added to V_S . [12] suggests that V_b is generated due to inherent imperfection of the analogue to digital converter (A/D in Fig 1) and dielectric leakage of the piezoelectric actuator. This bias voltage enters the digital controller together with V_S. Tiny bias voltage is accumulated through integration and significantly affects the calculated charge within the digital controller. Thus, the estimated charge ($\hat{q}_P$) does not equal the real charge across the actuator (q_P). This phenomenon, depicted in Fig.2, is called drift [12]:

$$\hat{q}_P = \int \frac{V_S + V_b}{R_s}\, dt \neq \int \frac{V_S}{R_s}\, dt \simeq q_P. \tag{3}$$

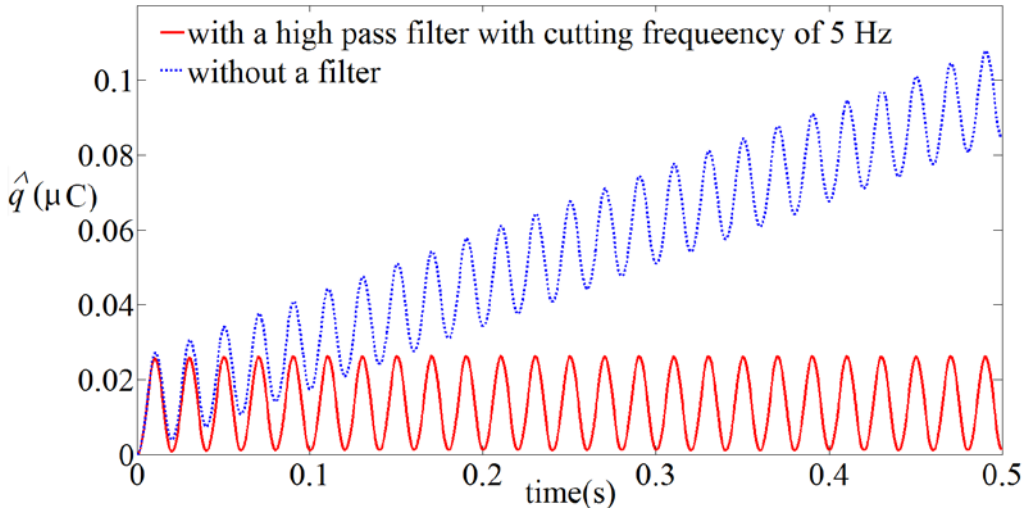

Figure 2. Estimated charge of a piezoelectric stack actuator excited by voltage of Ve =12sin(50*2π)t+12 V. Length and capacitance of the stack are 10 mm and 1.046 μF. RS =137.9 Ω and filter cutting frequency is 5 Hz

Role of the high pass filter in Fig.1 is to remove the bias voltage to avoid drift, as shown in Fig.2. With use of a high pass filter with a high enough cutting frequency (e.g. 5 Hz for the actuator detailed in the legend of Fig. 2), a realistic estimation of charge/position is achievable.

2- A Design Guideline for CEPASR

In this research, two rough design objectives of O1 and O2 are considered for CEPASRs:

O1- high precision

O2- low voltage drop

Resolution and input voltage range of A/D units of an I/O card play the major role in precision. Each A/D unit has *n* bits (resolution) and one or a number of range(s) for input voltage. For instance, an A/D may have 12 bits and its input range could be chosen from three options of ±0.625 V, ±2.5 V and ±10 V. Then, 2^n digital numbers is allocated to the input range of choice [27]. The larger portion of the range covered by the input voltage (signal), the more digital numbers used to quantify the input signal, the higher precision. Hence, for a given resolution, maximum precision is achieved if input range of an A/D is fully used. V_S is the input to the A/D in digital charge estimators as depicted in Fig.1. Therefore, to achieve the highest precision, the range of V_S should be equal to an input range of the A/D of the I/O card; this is a guideline to achieve O1.

Voltage drop, the portion of V_e not used for actuation, equals V_S. Thus, V_S can replace voltage drop in O2. Hence, V_S should be as small as possible; this is a guideline to attain O2.

In summary, for a given A/D, design objectives of O1 and O2 result in following design guidelines:

G1- The range of V_S should be equal to an input range of the A/D.

G2- V_S should be as small as possible.

For a given A/D, both G1 and G2 can be combined as «Design Guideline: the range of V_S should be equal to the smallest input range of the A/D».

This guideline guarantees the maximum precision at the smallest possible voltage drop. With a given excitation voltage (which depends on the required displacement) and A/D, R_S, in Fig. 3, is the only variable to tune V_S so as to meet the aforementioned guideline.

3- Adaptive CEPASR to Meet the Design Guideline

Figures 3 and 4 depict V_S for the estimator of Fig.1 with a 5×5× 36 mm Piezo Stack of SA050536 type made by PiezoDrive Company[28] and R_S=100 Ω and R_S=44 Ω respectively. The minimum input range of the A/D is ±0.625 V.. Figure 3 depicts the sensing voltage for excitation voltages of 10sin(20×2πt)+10 V and 10sin(50×2πt)+10 V with a phase of -90°. At the excitation frequency of 50 Hz, the selected value of R_S leads to use of a large portion of the input range and nearly fulfils the guideline. However, at 10 Hz, 55% of input range is left unused and the guideline is not met. Figures 4 shows the sensing voltage with two triangular excitation voltages with the identical pick to pick range of [0 20] V and frequencies of 20 Hz and 60 Hz. At the excitation frequency of 60 Hz, the input range is almost fully used and fulfils the design guideline. However, at the frequency of 20 Hz, 56% of input range is not used; thus, the guideline is not met

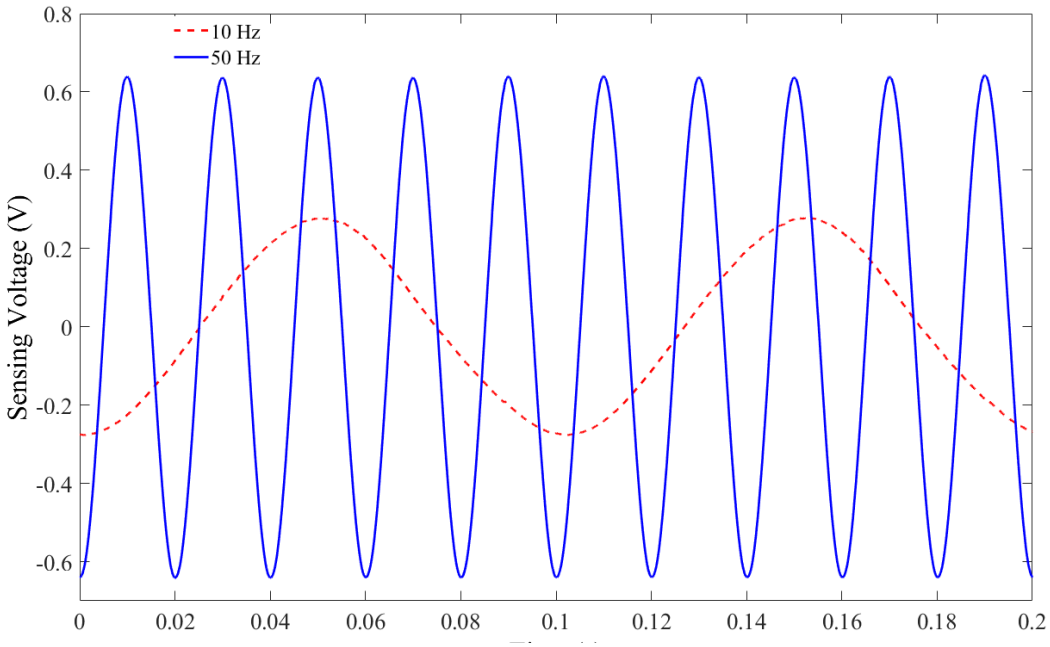

Figure 3. The range of sensing voltage fo sinusoidal excitation with same amplitude of 10 V and different excitation frequencies of 10 and 50 Hz. The actuator is PZT with dimensions of 5×5× 36 mm. The sensing resistor is 100 Ω.

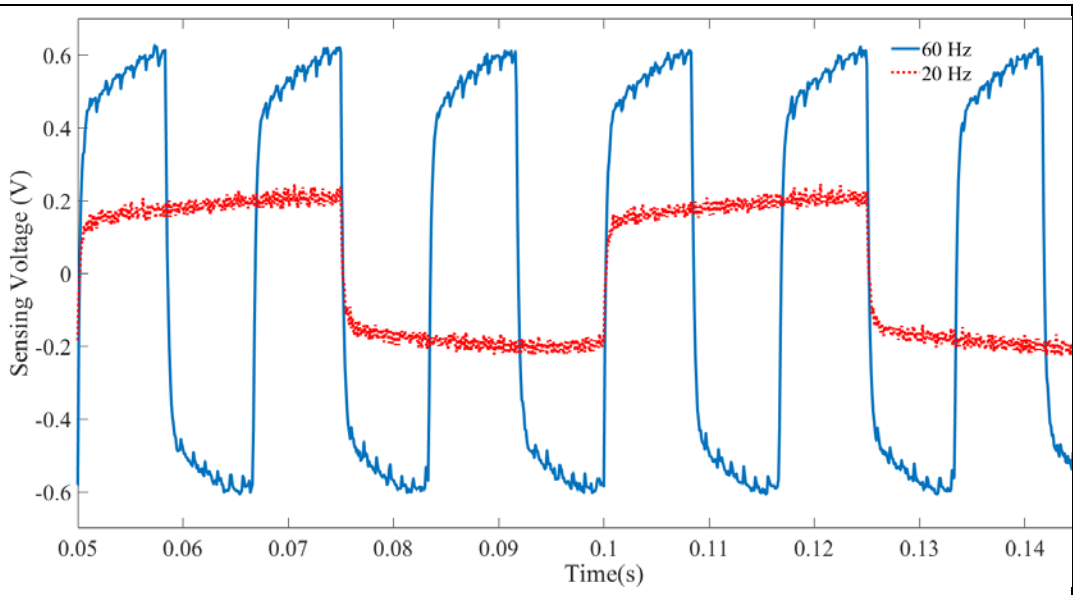

Fig. 4. The range of sensing voltage for same excitation range of 20 V and different excitation frequencies of 20 and 60 Hz. The actuator is PZT with dimensions of 5×5× 36 mm. The sensing resistor is 44 Ω.

Figures 3 and 4 shows that a CEPASR with a single value of R_S cannot satisfy the guideline across a wide area of operation. However, all reported digital charge estimators of piezo-actuated nanopositioning systems have either a single value [12, 25] or only a few instinctively chosen values of R_S [21]. This research, alternatively, proposes an adaptive charge estimator with operation-condition-dependent R_S. Such a charge estimator requires a mathematical model (F in (4)) to approximate the right R_S at any operating condition so as to fulfil the design guideline, i.e. to reach a desired V_S amplitude e.g. 0.625 V:

$$\hat{R}_S = F(\text{operating conditions}), \quad (4)$$

where operating conditions are waveform, amplitude (in V) and frequency(in Hz) of excitation voltage (V_e in Fig.1). Hat accent (^) refers to an approximated value. That is, (4) can be re-written as:

$$\hat{R}_S = F(V_e \text{ waveform}, V_e \text{ amplitude}, V_e \text{ frequency}) \quad (5)$$

4- Analytical Approximation of the Sensing Resistor to Realise Adaptive CEPASR

If the piezoelectric actuator is approximated by a capacitor, C_P [21] and minute current entering the A/D card is neglected, then, using Fig.1, the combination of actuator and sensing resistor can be depicted as Fig.5.

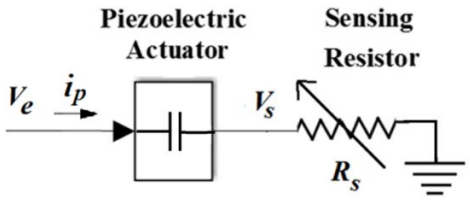

Figure 5. The major path of electrical current in a CEPASR, where the actuator is assumed equivalent of a capacitor

For such an approximate system, in Laplace domain,

$$i_P(s) = \frac{V_e(s)}{R_S + \frac{1}{C_P s}} = \frac{V_S(s)}{R_S} \quad . \tag{6}$$

As a result, the transfer function between the sensing voltage, V_S, and the excitation voltage, V_e, is

$$\frac{V_S(s)}{V_e(s)} = \frac{R_S C_P s}{R_S C_P s + 1}. \tag{7}$$

Two waveforms are considered for the excitation voltage, sinusoidal and triangular which are addressed separately.

4-1 Sinusoidal Excitation

For the approximate linear system presented by (7), a sinusoidal excitation voltage without a bias, $V_e = A_e \sin\omega t$, leads to a sensing voltage of $V_S = A_S (\sin\omega t + \phi)$, where the amplitude of A_S and A_e have the following relationship:

$$\frac{|V_S|}{|V_e|} = \frac{A_S}{A_e} = \left| \frac{R_S C_P j\omega}{R_S C_P j\omega + 1} \right| = \frac{R_S C_P \omega}{\sqrt{(R_S C_P \omega)^2 + 1}} \Rightarrow A_S \sqrt{(R_S C_P \omega)^2 + 1} = A_e R_S C_P \omega$$

$$\Rightarrow A_S{}^2 \left((R_S C_P \omega)^2 + 1 \right) = A_e{}^2 (R_S C_P \omega)^2 \Rightarrow (R_S C_P \omega)^2 \left(A_e{}^2 - A_S{}^2 \right) = A_S{}^2.$$

Consequently,

$$\hat{R}_S = \frac{A_S}{C_P \omega \sqrt{A_e{}^2 - A_S{}^2}}, \tag{8}$$

For the I/O card of this research, A_S=0.625 V. In addition, for a 5×5×10 mm^3 piezoelectric stack actuator, used in this research, C_P =1.046 μF and respectively. Therefore,

$$\hat{R}_S = \frac{0.5975 \times 10^6}{\omega \sqrt{A_e{}^2 - 0.390625}}, \tag{9}$$

where the unit for R_S is Ω. For A_e>>1,

$$\hat{R}_S \simeq \frac{0.6 \times 10^6}{A_e \omega} = \frac{0.95 \times 10^5}{A_e f}, \tag{10}$$

where ω is frequency in rad/s, and f is in Hz. (10) clearly shows that the excitation amplitude and frequency has an effect on choice of the sensing resistor so promotes the idea of having varying sensing resistors in CEPASRs. Equations (9 and 10) are valid only for the case study of this paper.

4-2 Effect of Bias

With approximation of the actuator as a capacitor, the charge estimator would be linear, and superposition could be performed. As a result, for a sinusoidal excitation

with bias of B, V_e= $|V_e|$ sinωt+ B, the sensing voltage can be assumed as sum of two components influenced by sinusoidal and fixed (bias) excitations.

A component of V_S which is only influenced by B is presented as V_{SB}. Final value of V_{SB} is shown to be zero:

$$V_{SB}(s) = \lim_{s\to 0} s \frac{R_S C_P s}{R_S C_P s + 1} \frac{B}{s} = 0. \tag{11}$$

That is, the effect of bias disappears shortly; hence, bias has no enduring effect.

4-3 Triangular Excitation

Let us assume the excitation voltage is a triangular wave with the frequency of $2\pi\omega$ Hz which is initially at its lowest pick of V_e= -A_S and increases up to V_e= -A_S . Using Fourier series,

$$V_e(\omega) = \frac{8A_e}{\pi^2} \sum_{n=1}^{\infty} \frac{-1}{(2n+1)^2} \sin\left((2n+1)\omega t + \frac{\pi}{2}\right) = \sum_{n=1}^{\infty} V_{es}(n), \tag{12}$$

where V_{es} is a sinusoidal component of V_e and $\left|V_{es}(n)\right| = \frac{8A_e}{\pi^2} \frac{-1}{(2n+1)^2}$.

For the approximate linear system presented by transfer function of (7), any excitation component of V_{es}(n)= $|V_{es}$(n)| sin$(2n+1)\omega t$ leads to a sensing voltage component of V_{Ss}= $|V_{Ss}|$ sin$((2n+1)\omega t+\phi_s)$, and

$$\begin{aligned} \left|V_{Ss}(n)\right| &= \left|\frac{R_S C_P j(2n+1)\omega}{R_S C_P j(2n+1)\omega + 1}\right| \left|V_{es}(n)\right| = \frac{R_S C_P (2n+1)\omega}{\sqrt{\left(R_S C_P (2n+1)\omega\right)^2 + 1}} \left|V_{es}(n)\right| \\ &\simeq R_S C_P (2n+1)\omega \left|V_{es}(n)\right| = \frac{8A_e}{\pi^2} \frac{-1}{2n+1} R_S C_P \omega. \end{aligned} \tag{13}$$

Due to superposition, $V_S(\omega) = \sum_{n=1}^{\infty} V_{Ss}$. (14)

Considering (12), (13) and (14),

$$V_S \simeq \frac{8A_e}{\pi^2} R_S C_P \omega \sum_{n=1}^{\infty} \frac{-1}{2n+1} \sin\left((2n+1)\omega t + \phi_s\right), \tag{15}$$

Interestingly, (15) is equal to Fourier series of a square wave with the frequency of $2\pi\omega$ Hz and amplitude of A_s :

$$A_S \simeq \frac{2A_e}{\pi} R_S C_P \omega. \tag{16}$$

Thus, R_S can be approximated as

$$\hat{R}_S \simeq \frac{A_S \pi}{2A_e C_P \omega}. \tag{17}$$

(17) is comparable with (8). For the case study of this paper, detailed in Experimental Setup and Problem Statement section, A_S=0.625 V and C_P =1.046 μF, then:

$$\hat{R}_S \simeq \frac{9.39\times10^5}{A_e\omega} = \frac{1.49\times10^5}{A_e f}, \tag{18}$$

where ω is frequency in rad/s and f is in Hz. Equation (18), similar to (10), shows the influence of excitation amplitude and frequency on the value of a well-selected sensing resistor; this influence supports the idea of having varying sensing resistors. (17) is general, while equation (18) is valid for the case study of this paper only. Both can be used for triangular excitations with picks of 0 and $2A_S$, because a bias (additional fixed voltage) has no enduring effect on response, as discussed in subsection 4-2.

5- Experimentations to Assess and Develop Sensing Resistor Approximators for Adaptive CEPASR

Figure 6 depicts the experimental setup. The digital controller is a personal computer equipped with MATLAB 8.6 /Simulink 8.6 software including Simulink Real-Time Desktop Toolbox 5.1. Two 5×5×36 mm^3 and 5×5×10 mm^3 piezoelectric stacks made by PiezoDrive Company [28], and the amplifier is AETECHRON 7114. A multifunctional card of Advantech PCI-1710U was employed to connect the computer and analogue parts. This card has a resolution of 12 bits and five optional A/D input ranges: ±10, ±5, ±2.5, ±1.25 and ±0.625 V.

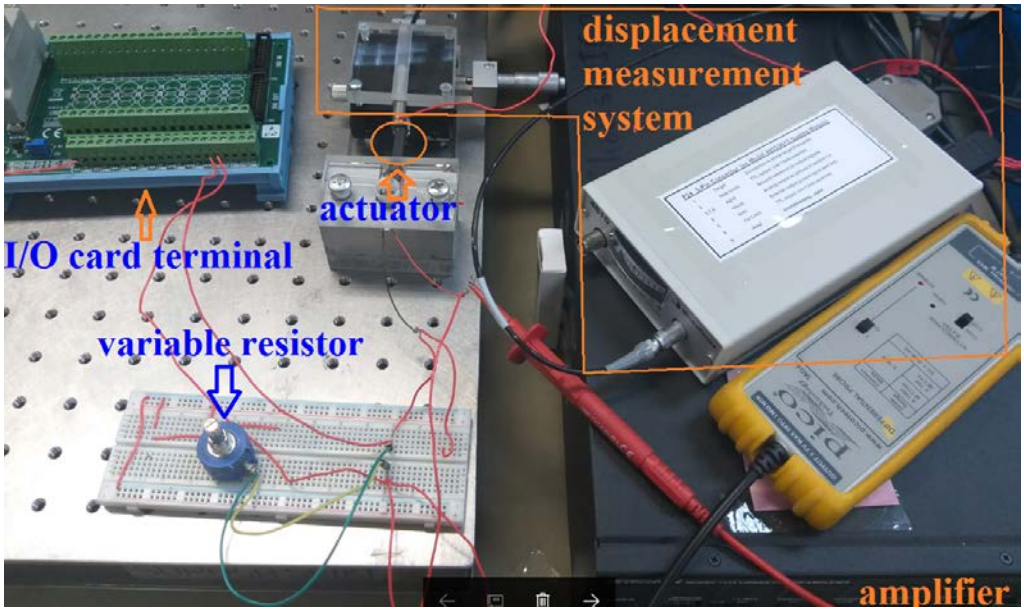

Fig. 6. Experimental setup, excluding the computer. Displacement sensor is not used in this research.

Four major series of experiments, including 112 experiments, were carried out. In all experiments, for a pair of amplitude and frequency, the sensing resistor was tuned so

that the sensing voltage just fits within the range of ±0.625, the smallest range of D/A. The recorded values of sensing resistance are the ones should be approximated by (5) or its more specific versions e.g. (10) and (18). All excitation voltages should be higher than 0 (due to practical limits of equipment); thus, in all experiments, a fixed voltage (bias) were added to the excitation voltage to increase the minimum voltage to 0.

Table 1. Experiments information

Excitation Function	$5\times5\times10$ mm^3 Stack	$5\times5\times36$ mm^3 Stack
Sinusoidal	Amplitudes (V):5,10,20,30,40	Amplitudes (V): 5, 7.5, 10, 12.5, 15,17.5
	Frequencies(HZ):20,30,40,50, 60,70,80	Frequencies(HZ):20,30, 40,50, 60,70,80
Triangular	Amplitudes (V):10,20,30	Amplitudes (V):5,10, 15, 20, 25
	Frequencies(HZ):20,30,40,50,60,70,80	Frequencies(HZ):20,30, 40,50, 60,70,80

6- Approximation of the Sensing Resistor to Realise Adaptive CEPASR

This section focuses on data-driven methods, in which most of them require data-driven model development. Development of a reliable data-driven model may include four tasks:

1- Mathematical Structure Definition
2- Parameter Identification
3- Overfitting Avoidance
4- Cross Validation

These tasks are performed with up to three separate data series, modelling, validation and test data.

In some models, the mathematical structure is not related only to the problem definition e.g. number of inputs and output and should be defined with use of modelling data. For instance, in a fuzzy model, the number of rules can be defined using the modelling data through subtractive clustering, or in exact RBFNs the size of the model depends on the modelling data.

Parameters of a data-driven model, with a known mathematical structure, are identified using the modelling data. Some models, e.g. linear and RBFN models, use single-step identification methods such as least square of errors (LSE) [29]. Others use iterative methods e.g. based on error propagation [30], where the parameters are tuned step by step to minimise the modelling error (also known as the training error, as detailed in Appendix A of [31]).

Overfitting refers to excessive focus on decrease of modelling error, which diminishes the generality of data-driven models [32, 33]. In iterative parameter

identification, such as in MLPs and FCC and neuro-fuzzy networks, at each iteration, the error is both calculated for the modelling and the validation data (the latter have not been used for parameter identification), a discrepancy in trend of these dual errors is considered as a sign of overfitting [31]. In models with single-step parameter identifications, e.g. RBFNs, some specific parameters are identified with validation data differently from the ones identified with modelling data to avoid overfitting [34].

Any data-driven model should fulfil the requirements of cross-validation. A widely accepted Monte-Carlo cross-validation criterion is that the estimation error of the model should be acceptable with test data, which is a series of data not used in model development [35].

Six types of data-driven models were developed in this research to approximate F in (5). They were used along with two other data-driven methods: averaging and cubic interpolation. In following subsections, a brief explanation of each model is presented with a focus on four aforementioned tasks for data driven modelling and use of modelling and validation data. In following subsections, y stands for the output, $\hat{R}_S$ and u_i is an input. According to (5), if excitation waveform (e.g. sinusoidal or triangular) is known, the remaining inputs are amplitude and frequency of excitation voltage.

6-1 Linear Models

In these models, the output is a linear combination of inputs:

$$y = \sum_{j=1}^{2} \mathbf{A}_i u_i + \mathbf{A}_{i+1}. \tag{19}$$

Nothing needs to be done to define the mathematical structure of this model (i.e. task 1 in the list of quadruple tasks at the beginning of section 6), as it is evident. Model parameters (elements of **A**) were identified with single-step method of LSE [29]. Overfitting was disregarded in development of (19) (i.e. task 3 was not performed); thus, both modelling and validation data were used for modelling.

6-2 Multi-layer Perceptrons (MLPs)

The employed MLPs have one hidden layer with m neurons and activation function of ϕ.

$$y = \sum_{j=1}^{m} \mathbf{B}_j \Psi\left(\sum_{i=1}^{2} \mathbf{C}_{ij} u_i + \mathbf{D}_i \right) + \mathbf{D}_{i+1}, \tag{20}$$

where

$$\Psi(x) = \frac{2}{1+\exp(-2x)} - 1. \tag{21}$$

MLPs, presented by (20) and (21), are universal approximators. That is, they have a proven capability to model any system when sufficient data are available [36, 37] .

In this research, m=2×*number of inputs*+1=5, (22), based on recommendation of [30]. m is the number of hidden layer neurons. As a result, mathematical structure is known. Parameter identification method uses the modelling data and is iterative. Validation data was used to avoid overfitting at each iteration. In this research, error back propagation with Levenberg-Marquardt algorithm [38] was utilised to identify

MLP parameters. In this method, some initial parameters may push the algorithm to be trapped in local minima of modelling error. Consequently, parameter identification should be repeated with different initial parameters. The model with the smallest error with validation data was chosen in the end.

6-3 Fully Connected Cascade (FCC) Networks

The employed FCC networks are very similar to the MLPs, with extra parameters (**E** elements) which connect the inputs directly to the output.

$$y = \sum_{j=1}^{5} \overline{\mathbf{B}}_j \Psi\left(\sum_{i=1}^{2} \overline{\mathbf{C}}_{ij} u_i + \overline{\mathbf{D}}_i \right) + \sum_{i=1}^{2} \mathbf{E}_i u_i + \overline{\mathbf{D}}_{i+1}. \tag{23}$$

FCC networks have shown their merit in solving some non-engineering benchmarks [39]. The number of hidden layer neurons, was considered same as the one of MLP, 5, as the same recommendation of (22) is valid for FCC networks too [39]. Role of modelling data and validation data for parameter identification, overfitting avoidance as well as evasion from local minima of error in FCC networks is similar to the ones of MLPs.

6-4 Neurofuzzy Networks

Linear Sugeno-type fuzzy models were used in this research which are convertible to neuro-fuzzy networks [40]. Such fuzzy models have *k* rules, each with *n* membership functions. For j^{th} rule and i^{th} input, the Gaussian membership function of (8) was employed to produce a membership grade, μ_{ij}, based on the input, u_i [41]:

$$\mu_{ij} = \exp\left(-\frac{(u_i - \mathbf{F}_{ij})^2}{2\mathbf{G}_{ij}^{\,2}} \right). \tag{24}$$

The product of membership grades of a rule was considered as the weight of the rule, a number between zero and one. The output of the whole model is the weighted sum of rules outputs [41]:

$$y = \frac{\sum_{j=1}^{k} \overbrace{\left(\sum_{i=1}^{n} \mathbf{H}_{ij} u_i + \mathbf{I}_j \right)}^{j^{th}\ rule\ output} \prod_{i=1}^{n} \mu_{ij}}{\sum_{j=1}^{k} \underbrace{\prod_{i=1}^{n} \mu_{ij}}_{j^{th}\ rule\ weight}}. \tag{25}$$

Neuro-fuzzy models, presented by (24) and (25), are universal approximators [42]. The mathematical structure of the fuzzy model, e.g. the number of rules (*k*), was defined through subtractive clustering (similar to [43]) with use of the modelling data. Modelling data were also used for iterative parameter identification. Validation data were used, at each iteration of parameter identification, to avoid overfitting.

6-5 Radial Basis Function Networks

RBFNs, which are universal approximators too [44], are presented as a combination of (26) and (27). They receive an array of inputs, $\mathbf{U}_{n\times w}$, rather than a set of inputs, u_i, i=1,…,n (n=2 in this research) .

$$\mathbf{O}_{ip} = \exp\left(-\left(\underbrace{S\sum_{j=1}^{n}\left(\mathbf{J}_{ij}-\mathbf{U}_{jp}\right)^2}_{\text{distance between input and weight arrays}}\right)^2\right). \quad (26)$$

$$\hat{\mathbf{Y}}_{1\times w} = \mathbf{K}_{1\times w}\times\mathbf{O}_{w\times w} + \mathbf{L}_{1\times w}. \quad (27)$$

In RBFN modelling, arrays of $\mathbf{J}_{w\times n}$, **K** and **L** and the scalar of S namely 'spread' should be identified.

In exact RBFNs, $\mathbf{J}=\mathbf{U_M}^T$ (28); where $\mathbf{U_M}^T$ is the transpose of an array of all inputs of modelling data. Thus, w equals the number of modelling data sets. For instance, in a modelling task of this research, $\mathbf{U_M}^T$ has the size of 2×30. In efficient RBFNs, with use of modelling data, the size of **J,** w, is defined through an algorithm which needs S as well as a target error, E_t, as detailed in [45]. As a result, the mathematical structure of RBFNs depends on modelling data.

RBFNs use a one-step parameter identification; hence, use of validation data to avoid overfitting after each iteration is inapplicable. Alternatively, the following pseudocode was utilised to tackle overfitting:

- For a range of S (and E_t)
    1. Find **J**, **K** and **L** with modelling data
    2. Find error with validation data (validation error)
- End
- Choice of S (and E_t) with minimum validation error

This algorithm generalises the RBFN modelling to some extent with use of validation data to calculate the error. Use of modelling data at line 2 would result in no generalisation; while, use of test data would violate the conditions of cross-validation.

6-6 Summary of Employed Data-driven Models

Table 2 summarises the tasks performed in development of each model and the data used for each task. MD and VD refer to modelling and validation data, respectively. Both two last rows refer to avoidance of overfitting through different strategies: (1) stopping parameter identification In the case of discrepancy in trend of modelling and validation error (used for MLP, FCC and neuro-fuzzy networks), and (2) use of extra parameters to improve generality of the models (used for RBFNs).

Table 2 Development stages for different models and their associated data

Model	Structure Definition	Parameter Identification	Over-fitting Avoidance-Stop Process	Over-fitting Avoidance-Extra Parameters
Linear		MD+VD		
MLP		MD	VD	
FCC		MD	VD	
Fuzzy	MD	MD	VD	
RBFN	MD	MD		VD

Results and Recommendations

This section first assesses the analytical model/approximator of the sensing resistance, then compares it with the developed FCC network. In the end, the risk of overestimation of R_S is discussed, and an alternative is presented to reduce this risk.

7-1 Analytical Model Results

Table 3 and Fig.7 presents experimental (real) sensing resistors, detailed in section 5, for a 5×5×10 mm^3 piezoelectric stack actuator and their associated estimated values by the analytical models of section 4. Fig.8 presents the same data a 5×5×36 mm^3 piezoelectric stack actuator for Table 1 also present the ratio of $r = R_S/\hat{R}_S$.

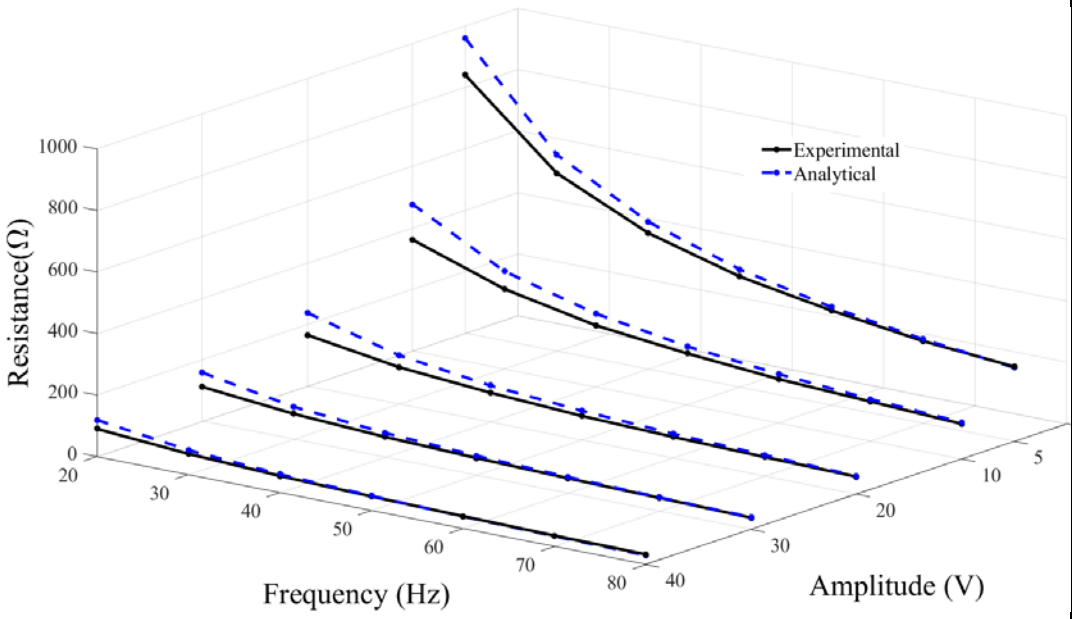

Figure 7. Experimental vs analytically-approximated sensing resistance for sinusoidal excitation and 5×5× 10 mm^3 stack piezoelectric actuator [24]

Table 3. Experimental and analytical estimated sensing resistances in Ω and their ratio, $r = R_S/\hat{R}_S$, for sinusoidal and triangular excitation voltages

Sinusoidal Excitation									
Amplitude	10V			20 V			30 V		
Frequency	$\hat{R}_S$	R_S	r	$\hat{R}_S$	R_S	r	$\hat{R}_S$	R_S	r
20	476	361	0.76	238	166	0.76	159	112	0.71
30	318	260	0.82	159	120	0.80	106	83	0.78
40	238	200	0.84	119	96	0.83	79	66	0.84
50	191	167	0.88	95	79	0.87	63	56	0.89
60	159	143	0.90	79	69	0.91	53	49	0.93
70	136	128	0.94	68	62	0.96	45	44	0.96
80	119	114	0.96	59	57	0.96	40	38	0.96
Triangular Excitation									
Frequency	$\hat{R}_S$	R_S	r	$\hat{R}_S$	R_S	r	$\hat{R}_S$	R_S	r
20	747	496	0.66	373	234	0.63	249	149	0.60
30	498	344	0.69	249	166	0.67	166	106	0.64
40	373	264	0.71	187	130	0.69	124	85	0.68
50	299	216	0.72	149	108	0.72	100	71	0.71
60	249	189	0.76	124	95	0.76	83	62	0.75
70	213	165	0.77	107	84	0.78	71	55	0.78
80	187	151	0.81	93	75	0.81	62	50	0.81

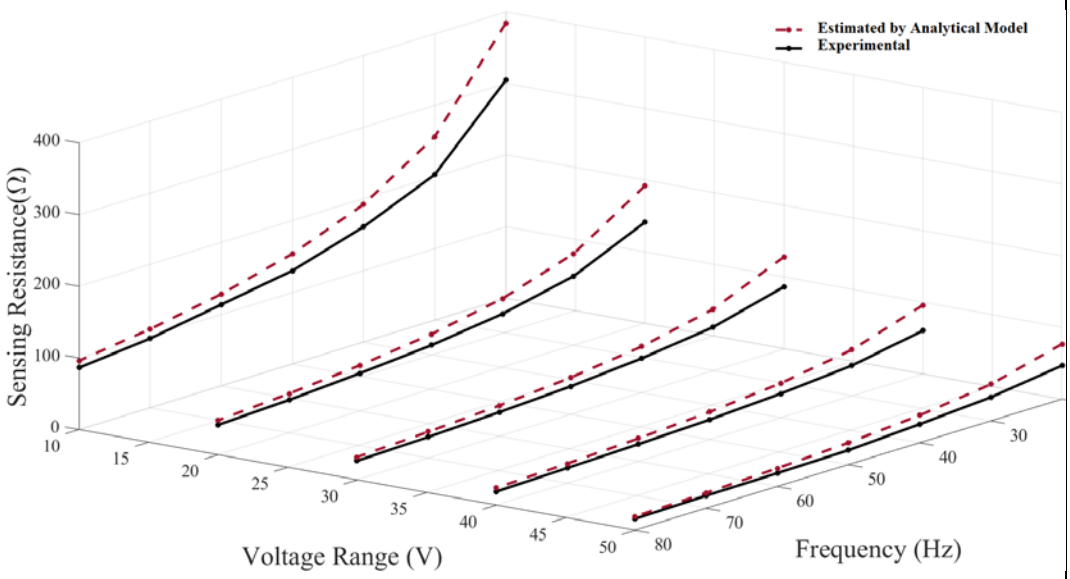

Fig. 8. Experimental vs analytically-estimated sensing resistances for triangular excitation and 5×5× 36 mm³ stack piezoelectric actuator

It is obvious that analytical models overestimate the resistance, particularly at low frequencies. These too high sensing resistances, if implemented, would lead to too high sensing voltages, surpassing the selected input voltage range of the A/D, i.e. ±0.625 V. As a result, the sensing voltage would be saturated and charge estimation cannot be performed in full.

7-2 Data-driven Approximators' Results

The data driven methods listed in Table 4 were carried out with use of the data presented in Table 1, for 5×5×10 mm^3 stack piezoelectric actuator and sinusoidal excitation. 25, 5 and 5 data sets were used as modelling, validation and test data, respectively. Both modelling and validation data were used in averaging and cubic interpolation. Amongst the methods listed in Table 4, for 4 test data sets, efficient RBFN shows superiority and for one test data set exact RBFN excels.

Table 4. Estimated Sensing Resistances by Different Models versus Experimental Values, for sinusoidal excitation of a 5×5×10 mm^3 stack piezoelectric actuator

Excitation Voltage (V)	R_S (Ω)	Estimated R_S (Ω)				
		Analytical Model	*Exact RBFN*	*Efficient RBFN*	*Cubic Interpolation*	*Averaging*
5 sin (2π×70*t*)	267.9	273.9	266.2	265.8	275.7	198.4
10 sin (2π×60*t*)	142.5	158.8	150.8	147.7	207.5	182.5
20 sin (2π×50*t*)	78.5	95.1	76.7	77.4	81.2	106.2
30 sin (2π×40*t*)	66.4	79.3	67.9	65.2	67.6	75.8
40 sin (2π×30*t*)	67.2	79.3	59.3	67.7	70.2	84.8

Table 5 compares the outputs of a FCC network (detailed in subsection 6-3) and the analytical model of section 4. The FCC netwrok were developed with use of the data presented in Table 1, for 5×5×36 mm^3 stack piezoelectric actuator and triangular excitation. 25 ,5 and 5 randomly selected data sets were used as modelling, validation and test data, respectively. Table 5 only includes five test data sets; as other 30 data sets have been used in development of the FCC network and match to this model extremely well.

Table 5. Sensing resistance approximation results for the analytical model and the FCC network for 5×5×36 mm^3 stack piezoelectric actuator and triangular excitation

	f (Hz)	Rs	$\hat{R}_S$		Relative Error%	
			Analytical	FCC Network	Analytical	FCC Network
5	70	96.5	109.7	94.8	13.7	-1.9
10	20	141.2	192.0	137.3	36.0	-2.8
15	60	33.5	42.7	35.2	27.3	5.0
20	50	27.6	38.4	25.9	39.1	-6.1
25	40	26.0	38.4	22.6	47.7	-13.1

The FCC network obviously outperforms the analytical model.

So far, it can be concluded that data-driven models of RBFN and FCC can outperform analytical models and statistical methods of averaging and interpolation.

Now, it is time to compare powerful data-driven models with each other. Table 6 presents the approximation performance for five data driven models detailed in section 6 . These models were developed with use of the data presented in Table 1, for 5×5×36 mm^3 stack piezoelectric actuator and sinusoidal excitation. 36 ,6 and 6 randomly selected data sets were used as modelling, validation and test data, respectively. MAE and MSE stand for mean of absolute error and mean of squared error.

Table 5 Different selection criteria for different models to approximate the sensing resistance, for sinusoidal excitation of a 5×5×36 mm^3 stack piezoelectric actuator

	MLP	FCC	Fuzzy	RBFN Efficient	RBFN Exact	Linear
MAE	0.623	1.386	2.652	1.537	2.000	54.916
Bias	0.127	1.265	0.370	1.070	-1.081	44.177
Variance	0.555	2.020	11.44	1.792	11.146	2682.8
MSE	0.571	3.620	11.58	2.937	12.315	4634.4
Number of Parameters	21	23	56	37	121	3

With attention to Tables 3-5. Table 5 shows the superiority of MLPs, detailed in subsection 6-2, over all other methods. MLP not only presents the smallest approximation error, bias and variance, but also, it has the second smallest number of parameters, after highly imprecise linear model.

7-3 Overestimation Avoidance

As detailed subsection 7-1, overestimation of the sensing resistor has a seriously damaging consequence, i.e. saturation of V_S (loss of V_S data at times); while, underestimation of R_S only results in decrease of precision, because it causes the range of V_S to be smaller than the smallest input range of A/D.

Assuming $(\hat{R}_S - R_S)$ has a Gaussian distribution, there is 50% chance of overestimation for any unbiased approximator (with B =0) [46]. (29) is suggested to be used to avoid overestimation of the sensing resistance (saturation of V_S).

$$\hat{R}_{SP} = \hat{R}_S - B - 3\sigma \,, \qquad (29)$$

where B is the bias and σ is the standard deviation of approximation. $\hat{R}_{SP}$ is practical approximated sensing resistance. According to [46], use of $\hat{R}_{SP}$ instead of $\hat{R}_S$ reduces the chance of overestimation of the sensing resistance to 1%.

Significance/Implications

1- Formulation of design procedure for charge estimators of piezoelectric actuators with sensing resistor, CEPASR, as one of the most recent key techniques in position control of piezoelectric actuators. This, for the first time, resulted in a design guideline to minimise voltage drop with maintaining maximum precision.

2- Finding analytical and data-driven methods to approximate sensing resistor in CEPASR. Eight different data-driven was compared to the analytical methods, and

multi-layer percepton (MLP) was found to be the best method to serve the aforementioned purpose.

Publications

Journal Papers

[1] M. Mohammadzaheri, M. Emadi, M. Ghodsi, E. Jamshidi, I. Bahadur, A. Saleem, M. Zarog "A variable-resistance digital charge estimator for piezoelectric actuators: an alternative to maximise accuracy and curb voltage drop," Journal of Intelligent Material Systems and Structures, vol. 30, pp. 1699-1705, 2019.

[2] M. Mohammadzaheri, M. Emadi, M. Ghodsi, E. Jamshidi, I. Bahadur, M. Zarog, A. Saleem" Development of a charge estimator for piezoelectric actuators, a radial basis function approach," International Journal of Artificial Intelligence and Machine Learning (in press)

[3] M. Mohammadzaheri, H. Ziaiefar, M. Ghodsi, E. Jamshidi, I. Bahadur, M. Zarog, M. Emadi, P. Soltani "Adaptive charge estimation of piezoelectric actuators with a variable sensing resistor", Sensors and Actuators, Physical A, submitted.

Conference Papers

[1] M. Mohammadzaheri, H. Ziaiefar;, M. Ghodsi, I. Bahadur;, M. Zarog, A. Saleem, M. Emadi "Adaptive Charge Estimation of Piezoelectric Actuators, a Radial Basis Function Approach," presented at the 20th International Conference on Research and Education in Mechatronics Wels, Austria, 23-24 May 2019.

[2] M. Mohammadzaheri, M. Emadi, H. Ziaiefar;, M. Ghodsi, I. Bahadur, M. Zarog " Data-driven modelling of engineering systems with small data, a comparative study of artificial intelligence techniques," presented at the 5th International Conference on Signal Processing and Intelligent Systems, Shahrood, Iran, 18-19 December 2019.

Conclusions

The target of this project was to design a precise sensorless nanopositioning system with use of piezoelectric actuators. Thus, expensive and troublesome position/displacement sensors should be replaced by precise position estimators. It is known, since 1980's, that for a wide operating area, charge of a piezoelectric actuator is proportional to its position. That is, a precise charge estimator can play the role of a displacement/position sensor. However, charge estimation of piezoelectric actuators has never been an easy task. This research made a major progress in this area.

The first practical charge estimator of piezoelectric actuators, for nanopositioning purposes, was introduced in 2006, with a capacitor in series with the actuator. However, in these systems, a large portion of the applied voltage is taken by the capacitor. This squandered voltage is called voltage drop. In 2010, with help of digital technology, a resistor (known as the sensing resistor) was suggested to replace the capacitor, and was shown to witness less voltage drop, compared to a an estimator with capacitor. However, all reported charge estimators of piezoelectric actuators with sensing resistor (CEPASRs) used a fixed instinctively chosen resistor for the entire

operating area. The literature does not offer any clear selection method for the sensing resistor. In this research, first, a guideline for selection of sensing resistor was identified, and then, it was experimentally shown that a fixed resistor cannot meet the identified guideline for a wide operating area. Consequently, it was concluded that adaptive CEPASR with operation-condition-related resistor should be designed.

Design of an adaptive CEPASR requires algorithms to approximate the sensing resistor so that the aforesaid resistor selection guideline is met. An analytical method as well as eight data-driven methods were employed to tackle this approximation problem. Mutli Layer Perceptrion (MLP), a type of artificial neural networks, outperformed other methods and was selected. In addition, a formulae was suggested to produce practical sensing resistance with only 1% chance to be higher than the apt sensing resistance.

(E) Project Achievement

List all the project objectives (as per the proposal) and what are the Achievements:

No.	Objective/Milestone	Achievements
1	Setting up a Nanopositioning Research Lab at Sultan Qaboos University	100%
2	Development of accurate position estimation algorithms, implementable on inexpensive digital devices	95%
3	Development of control systems, implementable on inexpensive digital devices, to be used jointly with the algorithms developed at stage 2	90%

(F) Challenges

Unexpected Events: *Please list and describe any unexpected events that occurred during the project that have negatively impacted your research.*

Description	Impact	Actions Taken
E.g. Equipment not arrived	*Experiment reschedule*	*Project extended*

(G) Research Output

Publications: *Please list all types of research publications that have arisen from the project.*

Type of Publication	**Status** (submitted/accepted/published)	**No. of Publication**
Journal Paper	**1 published, 1 accepted, 1 submitted**	**3**
Conference Paper	**1 published, 1 presented (in press)**	**2**
Book Chapter		
Book		
Other (please specify)		

Intellectual Property (IP): *Please list all types of intellectual properties that have arisen from the project.*

Type of IP	**Description**
Example: (Patents, process, machine, composition of matter, article of manufacture, copyright, know-how, new devices, chemical compound, etc.)	

Organization of Events: *Please list all types of events that have been organized as a result of the project. (If applicable)*

Type of Event	**Title of the event**	**Month/Year**
Workshop		
Exhibition		
Conference/ Symposium		
Short Course		
Seminar		
Other (please specify)		

Dissemination to Professional Events and Society: *Please list all dissemination that has occurred at professional events or for wider society as a result of the project. (If applicable)*

Type of Event	**Description**	**Month/Year**
Media		
Public Presentation		
Other (please specify)		

Deliverables to Beneficiaries: *Please list all deliverables that have arisen as a result of the project. (If applicable)*	
Beneficiary	**Deliverable**

(H) Research Collaboration

Please list all collaborations you have had with local/international institutions on personal or official levels as a result of the project. (*If applicable*)

Type of Collaboration (co-publications, co-funding, etc.)	**Collaborator (Person's Name/Organization/Country)**
(e.g. co-publications of peer review journal paper)	[Name], [Organization], [Country]

(I) Declaration

I declare all information in this report is correct.

Principal Investigator	
Name: Morteza Mohammadzaheri	**Signature & Date:**

(J) Approvals

For College Research Committee (CRC)/Research Center Committee (RCC) only

College Research Committee (CRC)/Research Center Committee (RCC) Decision	
Report Approved ☐	Revise the Report ☐
Comments:	
Name: **Position:**	**Signature & Stamp:** **Date:**

Note: If the report needs revision, the principal investigator should revise the report and resubmit it to the committee.

For Research Department only

Research Department Approval	
Name: **Position:**	**Signature & Stamp:** **Date:**

References

[1] G. M. Clayton, S. Tien, K. K. Leang, Q. Zou, and S. Devasia, "A review of feedforward control approaches in nanopositioning for high-speed SPM," *Journal of Dynamic Systems, Measurement, and Control,* vol. 131, p. 061101, 2009.

[2] Y. H. Teh, "Labview Based Pid Algorithm Development for Z Motion Control in Atomic Force Microscopy," UTAR, 2015.

[3] X. Li and C. C. Cheah, "Robotic cell manipulation using optical tweezers with unknown trapping stiffness and limited fov," *IEEE/ASME Transactions on Mechatronics,* vol. 20, pp. 1624-1632, 2015.

[4] S. Saedi, A. Mirbagheri, A. Jafari, and F. Farahmand, "A local hybrid actuator for robotic surgery instruments," *International Journal of Biomechatronics and Biomedical Robotics 33,* vol. 3, pp. 100-105, 2014.

[5] H. Tang, Z. Zeng, J. Gao, and X. Zhang, "A flexible parallel nanopositioner for large-stroke micro/nano machining," in *International Conference on Manipulation, Manufacturing and Measurement on the Nanoscale (3M-NANO)*, 2015, pp. 107-110.

[6] V. Protopopov, "Beam Alignment and Positioning Techniques," in *Practical Opto-Electronics*, ed: Springer, 2014, pp. 309-334.

[7] M. Ghodsi, A. Saleem, A. Özer, I. Bahadur, K. Alam, A. Al-Yahmadi, *et al.*, "Elimination of thermal instability in precise positioning of Galfenol actuators," in *Behavior and Mechanics of Multifunctional Materials and Composites* 2016, p. 980008.

[8] L. Díaz Pérez, M. Torralba Gracia, J. Albajez García, and J. Yagüe Fabra, "One-Dimensional Control System for a Linear Motor of a Two-Dimensional Nanopositioning Stage Using Commercial Control Hardware," *Micromachines,* vol. 9, p. 421, 2018.

[9] M. Mohammadzaheri and A. AlQallaf, "Nanopositioning systems with piezoelectric actuators, current state and future perspective," *Science of Advanced Materials,* vol. 9, pp. 1071-1080, 2017.

[10] S. O. R. Moheimani, "Invited Review Article: Accurate and fast nanopositioning with piezoelectric tube scanners: Emerging trends and future challenges," *Review of Scientific Instruments,* vol. 79, Jul 2008.

[11] N. Miri, M. Mohammadzaheri, and L. Chen, "An enhanced physics-based model to estimate the displacement of piezoelectric actuators," *Journal of Intelligent Material Systems and Structures*, p. 1045389X14546648, 2014.

[12] M. Bazghaleh, M. Mohammadzaheri, S. Grainger, B. Cazzolato, and T. F. Lu, "A new hybrid method for sensorless control of piezoelectric actuators," *Sensors and Actuators A: Physical,* vol. 194, pp. 25-30, 2013.

[13] M. Mohammadzaheri, R. Tafreshi, M. Mohammad-khorasani, M. Bazghaleh, and S. Grainger, "Evaluation of the induced voltage in driven electrodes of piezoelectric tube actuators for sensorless nanopositioning," in *IEEE 8th GCC Conference and Exhibition* 2015, pp. 1-5.

[14] M. Bazghaleh, S. Grainger, and M. Mohammadzaheri, "A review of charge methods for driving piezoelectric actuators," *Journal of Intelligent Material Systems and Structures,* vol. 29, pp. 2096-2104, 2018.

[15] H. Ahmadpour, M. Mohammadzaheri, M. Emadi, V. Ghods, D. Mehrabi, and R. Tafreshi, "Neural Modelling of a Piezoelectric Actuator Inspired by the Presiach Approach," presented at the International Conference on Artificial Intelligence, Energy and Manufacturing Engineering Dubai, UAE, 2015.

[16] D. An, H. Li, Y. Xu, and L. Zhang, "Compensation of Hysteresis on Piezoelectric Actuators Based on Tripartite PI Model," *Micromachines*, vol. 9, p. 44, 2018.

[17] R. Barrett and C. Quate, "Optical scan-correction system applied to atomic force microscopy," *Review of Scientific Instruments*, vol. 62, pp. 1393-1399, 1991.

[18] K. A. Yi and R. J. Veillette, "A charge controller for linear operation of a piezoelectric stack actuator," *IEEE Transactions on Control Systems Technology*, vol. 13, pp. 517-526, 2005.

[19] M. Bazghaleh, S. Grainger, B. Cazzolato, and T.-f. Lu, "An innovative digital charge amplifier to reduce hysteresis in piezoelectric actuators," presented at the Australian Robotics and Automation Association (ACRA), Brisbane, Australia, 2010.

[20] J. Minase, T. F. Lu, B. Cazzolato, and S. Grainger, "A review, supported by experimental results, of voltage, charge and capacitor insertion method for driving piezoelectric actuators," *Precision Engineering*, vol. 34, pp. 692-700, 2010.

[21] M. Bazghaleh, S. Grainger, M. Mohammadzaheri, B. Cazzolato, and T. Lu, "A digital charge amplifier for hysteresis elimination in piezoelectric actuators," *Smart Materials and Structures*, vol. 22, p. 075016, 2013.

[22] C. Yang, C. Li, and J. Zhao, "A Nonlinear Charge Controller With Tunable Precision for Highly Linear Operation of Piezoelectric Stack Actuators," *IEEE Transactions on Industrial Electronics*, vol. 64, pp. 8618-8625, 2017.

[23] S.-T. Liu, J.-Y. Yen, and F.-C. Wang, "Compensation for the Residual Error of the Voltage Drive of the Charge Control of a Piezoelectric Actuator," *Journal of Dynamic Systems, Measurement, and Control*, vol. 140, pp. 1-9, 2018.

[24] M. Mohammadzaheri, M. Emadi, M. Ghodsi, E. Jamshidi, I. Bahadur, A. Saleem, *et al.*, "A variable-resistance digital charge estimator for piezoelectric actuators: An alternative to maximise accuracy and curb voltage drop," *Journal of Intelligent Material Systems and Structures*, vol. 30, pp. 1699-1705, 2019.

[25] M. Bazghaleh, S. Grainger, M. Mohammadzaheri, B. Cazzolato, and T.-F. Lu, "A novel digital charge-based displacement estimator for sensorless control of a grounded-load piezoelectric tube actuator," *Sensors and Actuators A: Physical*, vol. 198, pp. 91-98, 2013.

[26] M. Bazghaleh, S. Grainger, M. Mohammadzaheri, B. Cazzolato, and T.-F. Lu, "A novel digital charge-based displacement estimator for sensorless control of a grounded-load piezoelectric tube actuator," *Sensors and Actuators A: Physical*, 2013.

[27] N. Gray, "ABCs of ADCs," N. Semiconductor, Ed., ed, 2006.

[28] PiezoDrive. (2018). *PiezoDrive Products*. Available: https://www.piezodrive.com/

[29] M. Mohammadzaheri, L. Chen, A. Ghaffari, and J. Willison, "A combination of linear and nonlinear activation functions in neural networks for modeling a de-

superheater," *Simulation Modelling Practice and Theory,* vol. 17, pp. 398-407, 2009.

[30] S. Haykin, *Neural Networks A Comprehensive Introduction*. New York, USA: Prentice Hall, New Jersey, 1999.

[31] M. Mohammadzaheri, R. Tafreshi, Z. Khan, M. Ghodsi, M. Franchek, and K. Grigoriadis, "Modelling of petroleum multiphase flow in electrical submersible pumps with shallow artificial neural networks," *Ships and Offshore Structures,* pp. 1-10, 2019.

[32] M. Mohammadzaheri, A. Mirsepahi, O. Asef-afshar, and H. Koohi, "Neuro-fuzzy modeling of superheating system of a steam power plant," *Applied Math. Sci,* vol. 1, pp. 2091-2099, 2007.

[33] G. C. Cawley and N. L. Talbot, "On over-fitting in model selection and subsequent selection bias in performance evaluation," *Journal of Machine Learning Research,* vol. 11, pp. 2079-2107, 2010.

[34] M. Mohammadzaheri, M. Ghodsi, and A. AlQallaf, "Estimate of the head of the head produced by electrical submeersible pumps on gaseous petroleum fluids, a radial basis function network approach," *International Journal of Artificial Intelligence and Applications,* vol. 9, pp. 53-62, 2018.

[35] A. Lendasse, V. Wertz, and M. Verleysen, "Model selection with cross-validations and bootstraps—application to time series prediction with RBFN models," *Artificial Neural Networks and Neural Information Processing—ICANN/ICONIP 2003,* pp. 174-174, 2003.

[36] T. P. Chen, H. Chen, and R. W. Liu, "Approximation capability in C(R^{-}N) by multilayer feedforward networks and related problems," *IEEE Transactions on Neural Networks,* vol. 6, pp. 25-30, Jan 1995.

[37] M. Mohammadzaheri, L. Chen, and S. Grainger, "A critical review of the most popular types of neuro control," *Asian Journal of Control,* vol. 16, pp. 1-11, 2012.

[38] M. Mohammadzaheri and L. Chen, "Intelligent predictive control of a model helicopter's yaw angle," *Asian Journal of Control,* vol. 12, pp. 667-679, 2010.

[39] D. Hunter, H. Yu, M. S. Pukish III, J. Kolbusz, and B. M. Wilamowski, "Selection of proper neural network sizes and architectures—A comparative study," *IEEE Transactions on Industrial Informatics,* vol. 8, pp. 228-240, 2012.

[40] M. Ahmadpour, W. L. Yue, and M. Mohammadzaheri, "Neuro-fuzzy Modelling of Workers Trip Production," in *32nd Australasian Transport Research Forum, ATRF 2009*, 2009.

[41] M. Mohammadzaheri, A. Firoozfar, D. Mehrabi, and M. Emadi, "A Fuzzy Virtual Temperature Sensor for an Irradiative Enclosure," in *ICTEA: International Conference on Thermal Engineering*, 2017.

[42] H. Ying, *General Takagi-Sugeno fuzzy systems are universal approximators*, 1998.

[43] M. Mohammadzaheri, S. Grainger, and M. Bazghaleh, "Fuzzy modeling of a piezoelectric actuator," *International Journal of Precision Engineering and Manufacturing,* vol. 13, pp. 663-670, 2012.

[44] J. Park and I. W. Sandberg, "Approximation and radial-basis-function networks," *Neural computation,* vol. 5, pp. 305-316, 1993.

[45] M. Mohammadzaheri, H. Ziaiefar, M. Ghodsi, I. Bahadur, M. Zarog, A. Saleem, *et al.*, "Adaptive Charge Estimation of Piezoelectric Actuators, a Radial Basis Function Approach," in *2019 20th International Conference on Research and Education in Mechatronics (REM)*, 2019, pp. 1-6.

[46] D. C. Montgomery and G. C. Runger, *Applied statistics and probability for engineers*: John Wiley and Sons, 2014.